Article

Salicylic Acid Conjugate of Telmisartan Inhibits Chikungunya Virus Infection and Inflammation

Rudra Narayan Dash,[○] Amrita Ray,[○] Prabhudutta Mamidi,[○] Saikat De, Tapas K Mohapatra, Alok K Moharana, Tathagata Mukherjee, Soumyajit Ghosh, Subhasis Chattopadhyay, Bharat B Subudhi,* and Soma Chattopadhyay*

Read Online

ACCESS | Metrics & More | Article Recommendations | SI Supporting Information

ABSTRACT: There is no approved antiviral for the management of the Chikungunya virus (CHIKV). To develop an antiviral drug that can manage both CHIKV and arthritis induced by it, an ester conjugate of telmisartan (TM) and salicylic acid (SA) was synthesized (DDABT1). It showed higher potency (IC$_{50}$ of 14.53 μM) and a good selectivity index [(SI = CC$_{50}$/IC$_{50}$) > 33]. On post-treatment of DDABT1, CHIKV infection was inhibited significantly by reducing CPE, viral titer, viral RNA, and viral proteins. Further, the time of addition experiment revealed >95% inhibition up to 4hpi indicating its interference predominantly in the early stages of infection. However, the late stages were also affected. This conjugate of SA and TM was found to increase the antiviral efficacy, and this might be partly attributed to modulating angiotensin II (Ang II) receptor type 1 (AT1). However, DDABT1 might have other modes of action that need further investigation. In addition, the in vivo experiments showed an LD$_{50}$ of 5000 mg/kg in rats and was found to be more effective than TM, SA, or their combination against acute, subacute, and chronic inflammation/arthritis in vivo. In conclusion, DDABT1 showed remarkable anti-CHIKV properties and the ability to reduce inflammation and arthritis, making it a very good potential drug candidate that needs further experimental validation.
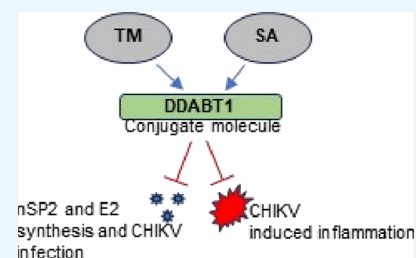
1. INTRODUCTION

Infection by CHIKV is characterized by fever, myalgia, and polyarthralgia in the acute phase. The acute symptoms subside gradually, but the symptoms of polyarthritis prolong to the postacute phases and may last for 90 days.[1,2] It is also associated with chronic comorbidities including tenosynovitis, tendinitis, and neuritis.[2,3] Since it has gradually become a global pathogen[4] and is no longer tropical, it cannot be neglected. However, there is no specific antiviral for it. Efforts to develop a new antiviral strategy for CHIKV have made very little progress because of many issues including lack of in vivo efficacy and poor selectivity.[5]

Viral inflammations are usually mediated by activation of angiotensin II (Ang II) receptor type 1(AT1) for Western equine encephalitis virus, neuroadapted Sindbis virus,[6] Dengue virus,[7] and Influenza A (H7N9) virus.[8] Recently, its involvement was demonstrated in CHIKV infection/inflammation,[9] where AT1-blocker [Telmisartan (TM)] was found to reduce CHIKV infection through modulation of the AT1/PPAR-γ/MAPKs pathways as well as targeting CHIKV-nsP2 (protease) in vitro.[9,10] Salicylic acid (SA) is known to activate multiple antiviral defense mechanisms in plants.[11] However, the antiviral properties of SA in humans are not known. Nevertheless, its prodrug (acetylsalicylic acid) has been shown to be effective against RNA viruses including influenza A and H1N1.[12] The effect of these salicylates on CHIKV infection is

not clear. Nonetheless, salicylates are known to reduce arthritis, which is the major symptom of CHIKV. Thus, a conjugate of TM and SA may reduce CHIKV infection and manage arthritis. Hence, in the current investigation, an ester conjugate (DDABT1) of TM with SA was developed and evaluated against CHIKV infection in vitro as well as assessed to control inflammation/arthritis in vivo.

2. MATERIALS AND METHODS

2.1. Chemicals, Drugs, Cells, Viruses, and Antibodies. Benzyl alcohol, carbon tetrachloride, sodium bicarbonate, N,N′-dicyclohexylcarbodiimide (DCC), and Complete Freund's adjuvant (CFA) were purchased from Sigma Chemicals Company, St. Louis, USA. Magnesium sulfate, ethyl acetate, dichloromethane, ethanol, and methanol were procured from Merck Chemicals, Mumbai (India), and carrageenan was purchased from Hi-media laboratories (Nashik, India). Pure TM was obtained as a gift (Torrent Research Center, Gandhinagar, India). Odisha Drugs and

Chemical Ltd., Bhubaneswar, India, gifted pure diclofenac and salicylic acid for this study. Other consumables were procured from local vendors. Binary gradient HPLC (Shimadzu, Japan with LC-20AD pump, SPD-M20A prominence diode array detector and 20 μL sample injection loop), Nylon-66 membrane filter (0.22 μm), Hamilton SYR 25 μL syringe (Alabama, USA), and Unisphere Aqua C18 (4.6 × 150 mm, 3 μm) analytical column (Agela Technologies, CA, USA) were used for chromatographic analysis. The sophisticated analytical instrument facility (SAIF) of CDRI, Lucknow, India, was availed for mass spectroscopy (Agilent 6520 Q-TOF ESI-HRMS & APCI-HRMS, CA.USA) and NMR spectroscopy (ADVANCE − 400 MHz, Bruker, Fällanden, Switzerland). The FT/IR-6000 spectrometer (Jasco, Tokyo, Japan) was used to record the IR spectrum.

CHIKV prototype strain (PS, accession no. AF369024.2) and CHIKV-E2 monoclonal antibody were gifted by Dr. M. M. Parida, DRDE, Gwalior, India. Dulbecco's modified Eagle's medium (DMEM; PAN Biotech, Aidenbach, Germany) supplemented with 5% fetal bovine serum (FBS, PAN Biotech, Aidenbach, Germany), gentamycin, penicillin, and streptomycin (PAN Biotech, Aidenbach, Germany) was used to maintain the Vero cell line (NCCS, Pune). The reagent [Val5]-angiotensin II acetate salt hydrate (Sigma-Aldrich, MO, US) was defined as AG. The anti-CHIKV-nsP2 monoclonal antibody was developed by us,[13] AT1 from Santa Cruz Biotech (TX, US), and GAPDH from Abgenex India Pvt. Ltd. (Bhubaneswar, India). Antibodies were procured from different companies.

2.2. Synthesis and Characterization of 2-((4′-((1,7′-Dimethyl-2′-propyl-1H,3′H-[2,5′-bibenzoimidazol]-3′-yl)methyl)-[1,1′-biphenyl]-2-carbonyl)oxy)benzoic Acid (DDABT1). In the first step, benzyl salicylate was prepared following the reported protocol.[14] The ester conjugate was prepared by reaction of benzyl salicylate with TM following a little modification of methods (Figure S1).[15] Following purification, in column chromatography (n-hexane: ethyl acetate, 4:6 v/v), the purity (96.5%) of (Figure S2) was ascertained by HPLC with methanol as mobile phase at a flow rate of 0.5 mL/min. This was then characterized as follows. Yield 66%, whitish in color, melting point 140 °C. FTIR (cm^{-1}): 3468.92 (OH-str), 2858.91 (CH-str), 1663.19 (C=O-str), 1241.24 (CO-str.).[1] H NMR (δ, ppm): 1.159 (d, CH$_3$), 1.686 (m, CH$_2$), 2.816 (m, CH$_2$), 3.768 (s, CH$_3$), 7.861 (m, Ar). ^{13}C NMR (δ, ppm): 26.1 (CH$_3$), 26.6 (CH$_3$), 34.7 (CH$_2$), 48.78 (CH$_2$), 48.907 (CH$_3$), 49.515 (CH$_2$), 173.64 (C=O), 163.299 (C=O), 136.7 (C=N), 131.659 (Ar−C−O), 131.374 (Ar), 120.182 (Ar), 118.246 (Ar), 113.98 (Ar). Mass (m/z): [M] calcd. for C$_{40}$H$_{34}$N$_4$O$_4$ 634.7 g/mol; found, 634.5; [M − 1$^+$] calcd 633.7 g/mol, found 633.5.

2.3. CHIKV Infection. Confluent Vero cells (90% confluency) seeded in 35 mm cell culture dishes (TPP, Trasachingen, Switzerland) were infected with CHIKV (PS strain) with a multiplicity of infection (MOI 0.1).[16,17] Infection was performed for 90 min. Then the plates were washed thrice with 1× PBS and fresh complete media (DMEM) was added. Infected cells were examined under a microscope (magnification, 10×) and bright-field images were taken at 18 hpi for the detection of the cytopathic effect (CPE). The cells and supernatants were harvested at 18 hpi to assess the expressions of viral RNA by qRT-PCR and viral structural and non-structural proteins by Western blot.

2.4. Cellular Cytotoxicity Assay. A 96-well plate (Corning) was used to seed the Vero cells (Approximately, 30,000 Vero cells/well). At 90% confluency, the cells were incubated with different concentrations (from 100 to 1000 μM) of DDABT1, TM, and SA (24 h at 37 °C in a CO$_2$ incubator). The cellular cytotoxicity was assessed by the MTT assay following the reported method.[18]

2.5. qRT-PCR. Vero cells were infected with CHIKV-PS strain (MOI 0.1) as mentioned above, and 100 μM DDABT1 was added postinfection. DMSO was used as a reagent control. The cells were harvested at 18 hpi and total RNA was extracted using Trizol (Invitrogen, MA, US).[9] Next, cDNA synthesis was carried out with an equal amount of RNA using the first strand cDNA synthesis kit (Invitrogen, MA, US) and qRT-PCR was performed using specific primers for the CHIKV-E1 and nsP2 genes (Table S3) as mentioned earlier GAPDH was taken as an endogenous control.[19] The qRT-PCR was performed as described earlier.[22]

2.6. Western Blot. Briefly, virus-infected and drug treated cells were lysed and proteins were separated on 10% SDS-PAGE. Western blot was carried out as per the protocol described earlier.[9] The blots were probed with the nsP2 and E2 monoclonal antibodies as per earlier reports. The band intensities were quantified using the ImageJ software.[20]

2.7. Plaque Assay. The plaque assays were performed following the reported procedure to quantitate the infectious viral titer.[21] The bar diagram showing the number of plaques as plaque forming unit/mL (PFU/mL) was generated using the GraphPad Prism software.

2.8. Immunofluorescence Analysis. Vero cells were grown on glass coverslips infected as described above and processed for immunofluorescence as described before.[22] At 18 hpi, the cells were fixed with freshly prepared 4% paraformaldehyde (PFA) for 30 min at RT. The cells were then permeabilized with 0.5% Triton X-100 for 5 min. After 3 washes, the cells were blocked with 3% Bovine serum albumin (BSA; Sigma), and cells were incubated with anti-E2 mAb for 1h at RT. Next, the cells were incubated with AF-594 conjugated with antimouse antibody (1:750) for 45 min. Then, coverslips were mounted with an antifade (Invitrogen). Fluorescence microscopic images were acquired using the Leica TCS SP5 confocal microscope (Leica Microsystems, Heidelberg, Germany) using a 20× objective, and images were analyzed using the Leica application suite (LASX) software.[16]

2.9. Time of Addition. DDABT1 (100 μM) was added to the Vero cells at 0, 2, 4, 6, 8, 10, and 12 hpi following infection with CHIKV-PS (MOI 0.1). At 18 hpi, the supernatants were collected for determination of viral titer by plaque assay following the established procedure.[23]

2.10. Effect of Drug Before, During, and After Infection. To determine the effect of DDABT1 on the CHIKV-PS replication cycle, Vero cells were infected at an MOI of 0.1 for 90 min at 37 °C. DDABT1 was added 1 h before (pretreatment) or with the virus to the cells (during treatment) or 1.5 h after CHIKV-PS inoculation (posttreatment). For the pretreatment assay, cells were first incubated with DDABT1 at 37 °C for 1 h, followed by three washes with 1× PBS, and then infected with CHIKV-PS for 1.5 h. For the during-treatment assay, cells were simultaneously incubated with CHIKV-PS and DDABT1 for 1.5 h at 37 °C. Then, the mixture was removed, and the cells were washed three times with 1× PBS before fresh complete DMEM media was added to the cells. The molecule was not added at any other time. For
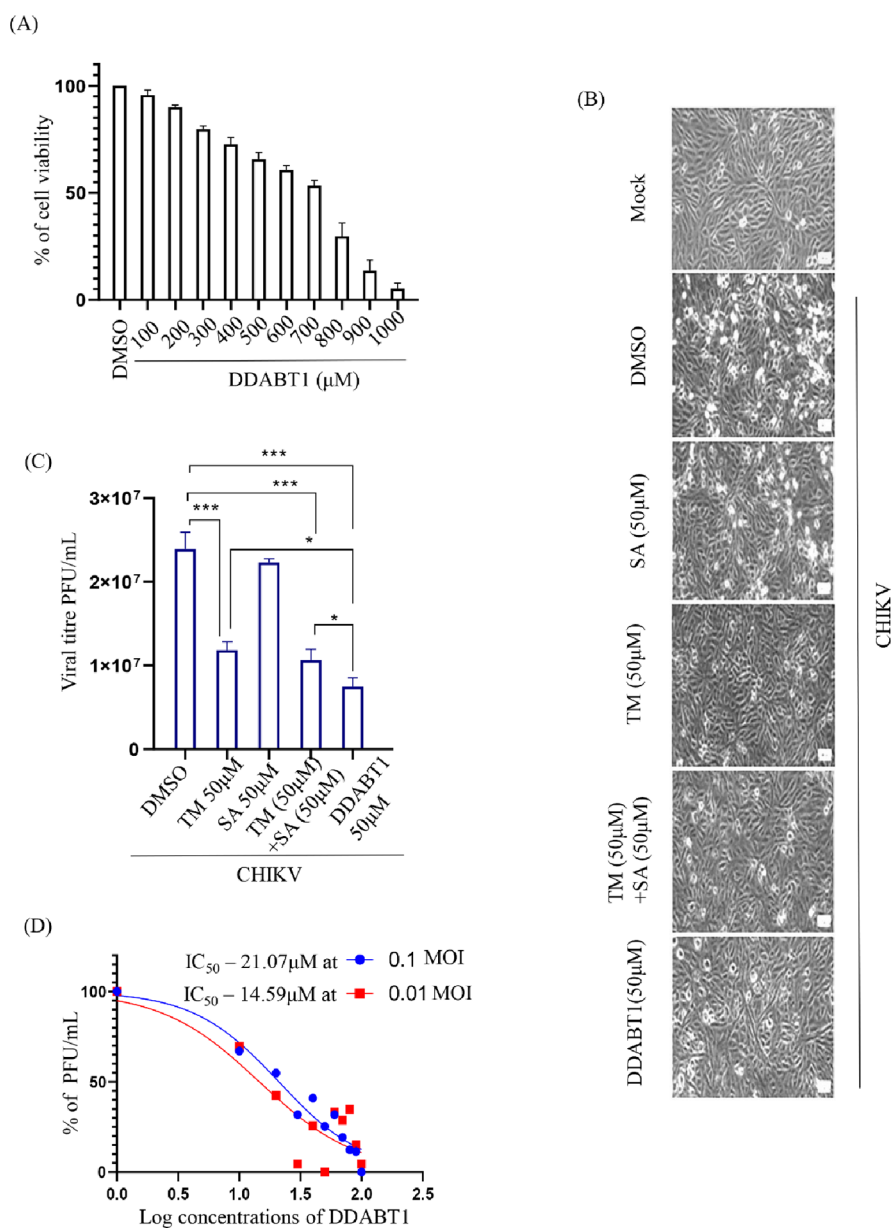
Figure 1. DDABT1 inhibits CHIKV infection more efficiently than TM: (A) Vero cells were treated with different concentrations of DDABT1 (100−1000 μM) and an MTT assay was performed as mentioned above. Bar graph showing the percent cellular viability of Vero cells with increasing concentration of DDABT1. (B) Morphological changes in cells induced during infection at 18 hpi as observed under microscope at 10× magnification. (C) Vero cells were infected with the CHIKV-PS strain of CHIKV (MOI 0.1) 50 μM doses of the drugs [TM/SA/TM + SA/ DDABT1], which were added separately to the infected samples. DMSO was used as vehicle control. The supernatants were harvested at 18hpi and plaque assay was carried out. Bar graph showing viral titers in drug-treated samples and control. (D) The Vero cells were infected with CHIKV-PS and different concentrations of DDABT1 were added. The supernatants were collected at 18 hpi and virus titers were determined by the plaque assay. The line diagram represents the IC50 value of DDABT1 in CHIKV-PS infected Vero cells, where the X-axis depicts the logarithmic value of the different concentrations of DDABT1 and the Y-axis depicts the percentage of PFU/mL. The statistical analysis of the experimental data was presented as mean ± SD of three independent experiments. *, $P \leq 0.05$; **, $P \leq 0.01$; ***, $P \leq 0.001$; and ****, $P \leq 0.0001$ were considered statistically significant.

the post-treatment assay, cells were infected with CHIKV-PS for 1.5 h, washed three times with 1× PBS, and then incubated with DDABT1 containing DMEM medium. In all three cases, the cells and supernatants were harvested at 18 hpi for assessing the expressions of viral RNA by qRT-PCR, viral structural and nonstructural proteins by Western blot, and viral titer by the plaque assay.[16]

2.11. Determination of Oral Acute Toxicity of DDABT1. The protocols for the oral acute toxicity study of DDABT1 were approved by the Institutional Animal Ethics Committee (1171/PO/Re/S/08CPCSEA) before use. Following the OECD-423 guidelines, a stepwise procedure (50, 300, and 2000 mg/kg) with three female Wistar albino rats (8−10 weeks old; 120−150 g) was used. The animals were fasted for approximately 15 to 16 h (with free access to water) before oral administration of a single dose of DDABT1 in 1% CMC with a dose volume of 10 mL/kg. Food was supplied approximately 3 to 4 h after administration of DDABT1, and the animals were kept under observation for toxicity/death. The results are summarized in Table S1.
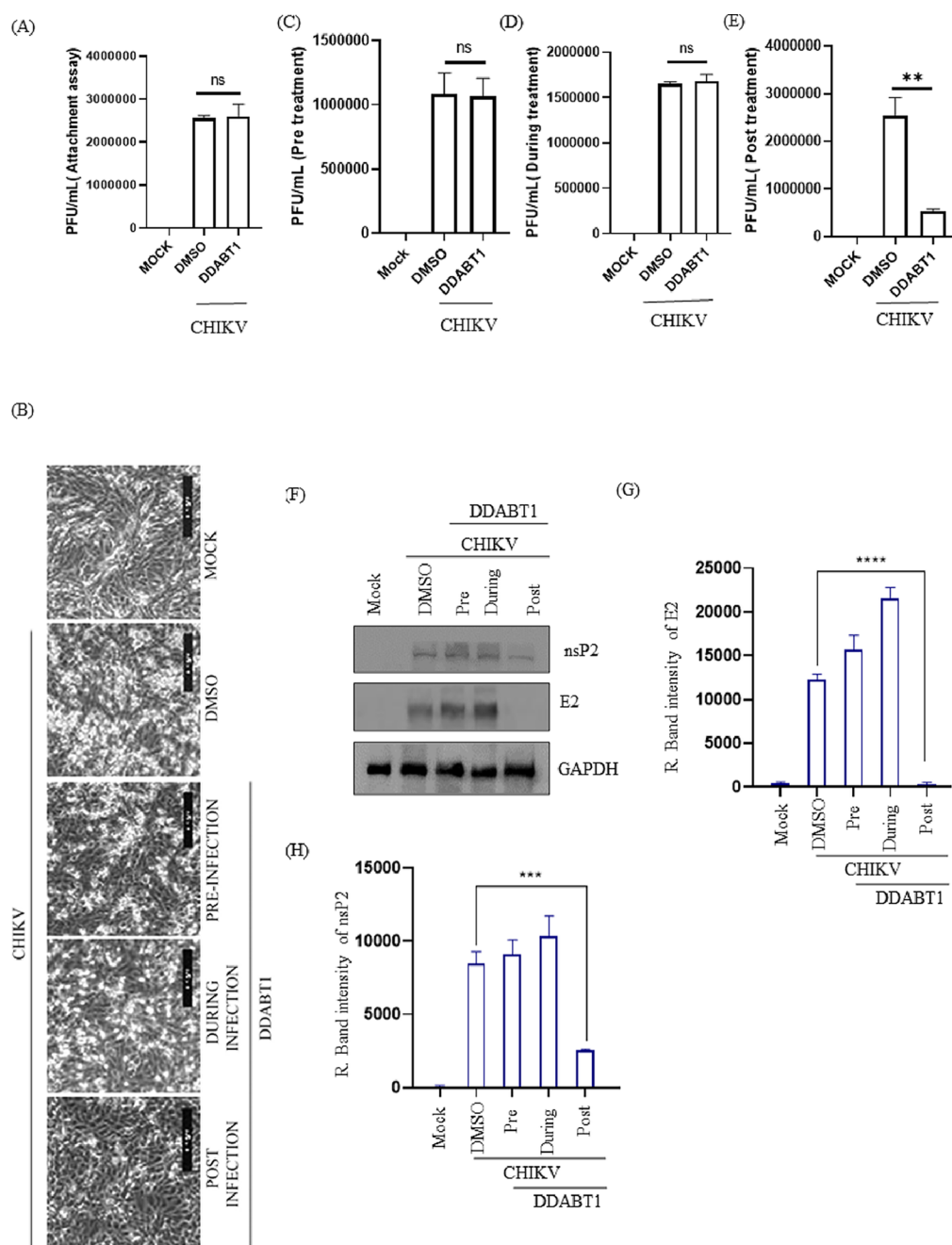
Figure 2. Post-treatment of DDABT1 reduces CHIKV infection significantly. (A) Before infection, the virus was incubated with 100 μM DDABT1 for 1 h [CHIKV + DDABT1]. Vero cells were then infected with CHIKV or preincubated CHIKV with 100 μM DDABT1 as mentioned above and supernatants were harvested at 18 hpi for estimating viral titers through the plaque assay. The bar graph shows the estimated viral titers in PFU/mL. (B) The Vero cells were treated with the compound (100 μm) separately before infection (1 h), during infection (1.5 h), and after infection (18 h). Pictures were taken with 10× magnification in a bright field microscope to show CPE. (C−E) Supernatants present in all three conditions were collected at 18 hpi and were subjected to the plaque assay. The bar diagram shows the percentage of viral titers in different conditions. (F) Cells were harvested at18 hpi and Western blot was performed using E2 and nsP2 specific mAb. GAPDH was taken as the loading control. (G, H) Bar diagram showing the relative band intensities of CHIKV E2 and nsP2. The statistical analysis of the experimental data was presented as mean ± SD of three independent experiments. *, $P \leq 0.05$; **, $P \leq 0.01$; ***, $P \leq 0.001$; and ****, $P \leq 0.0001$ were considered statistically significant.

2.12. Anti-Inflammatory Properties of DDABT1.

The acute anti-inflammatory activity was evaluated using established and approved protocols.[24] The Wistar rats (180−220 g) were used in this study. For this, six groups ($n = 6$) were treated with vehicle, diclofenac (10 mg/kg or 0.033 mmol/kg), SA (10 mg/kg or 0.724 mmol/kg po), TM (10 mg/kg or 0.0194 mmol/kg po), combination (SA 0.724 mmol/kg + TM 0.0194 mmol/kg p.o.), and DDABT1 (12 mg/kg or 0.0194

mmol/kg p.o.) 1 h prior to carrageenan injection (0.1 mL of 1% carrageenan solution) into the subplantar tissue of the left hind paw of each rat. A water plethysmometer was used to measure swellings of the paw at 1, 2, 3, and 4 h of injection. Assuming that the increase in the volume of paws of the control group of animals (no drug treatment) following carrageenan injection was 100%, the percentage of inhibition of paw-edema volume in test groups was determined.
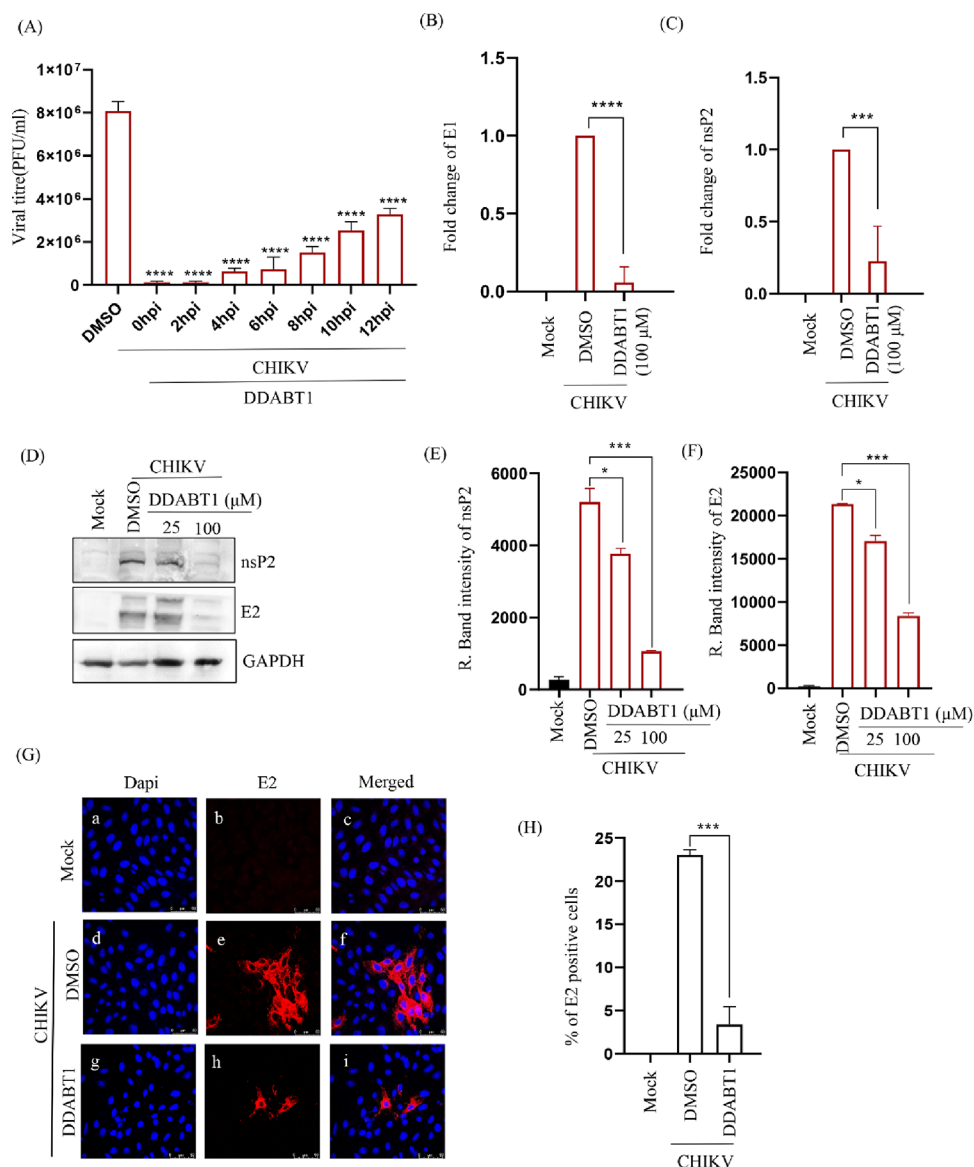
Figure 3. DDABT1 inhibits the CHIKV RNA and protein levels. (A) Vero cells were infected with CHIKV-PS (MOI 0.1) and DDABT1 (100 μM) was added at 0, 2, 4, 6, 8, 10, and 18 hpi. The CHIKV supernatants of all the experimental samples were harvested at 18 hpi and plaque assay was carried out. Bar graph depicting the viral titers in PFU/mL of all the drug-treated samples. DMSO was used as the vehicle control. The data represent the mean $\pm$ SD of three independent experiments. *$p < 0.05$ was considered to be statistically significant. Vero cells were infected with CHIKV-PS (MOI 0.1) and treated with DDABT1 (100 μM or 25 μM and 100 μM). (B, C) The cells were harvested at 18 hpi and total cellular RNA was isolated for amplifying the CHIKV E1 and nsP2 genes by qRT-PCR. (D) Cells were harvested and subsequently lysed in RIPA to perform Western blot using E2 and nsP2 specific mAbs where GAPDH was taken as the loading control. (E, F) Bar diagram demonstrating the relative band intensities of CHIKV E2 and nsP2, respectively. (G) The cells were fixed at 18 hpi and processed for the immunofluorescence assay to assess the protein levels of E2 using specific mAbs. (H) Graph depicting the % of E2 positive cells. The statistical analysis of the experimental data was presented as mean $\pm$ SD of three independent experiments. *, $P \leq 0.05$; **, $P \leq 0.01$; ***, $P \leq 0.001$; and ****, $P \leq 0.0001$ were considered statistically significant.

For evaluating the effect against subacute inflammation the cotton pellet-induced granuloma model in rats was used as per the method of D'Arcy et al.[25] Briefly, the region below the axilla of the rats was shaved and cleaned with 70% ethanol. Each sterile cotton pellet weighing 10 ± 1 mg was implanted subcutaneously (S.C.) in this region under light ether anesthesia. The animals were divided into six groups ($n = 6$). A control group of animals received only a vehicle, while the standard group of animals received diclofenac (0.033 mmol/kg p.o.). Similarly, test group-1 and test group-2 of animals received SA and TM at a dose of 0.724 and 0.0194 mmol/kg, respectively. Simultaneously, the test group-3 animal

received SA and TM in combination (0.724 + 0.0194 mmol/ kg), and finally, the animal of test group-4 received DDABT1 at a dose of 0.0194 mmol/kg. The drugs were given once daily for 7 days. On the eighth day, the animals were anesthetized with diethyl ether, and the pellets were removed carefully and freed from extraneous tissues. The pellets were weighed for wet weight and then dried in an oven at 60 °C until a constant weight was obtained. The measure of exudate formation = wet weight of pellet − dry weight of the pellet. The measure of granuloma tissue formation = dry weight − the initial dry weight of the pellet (10 mg).
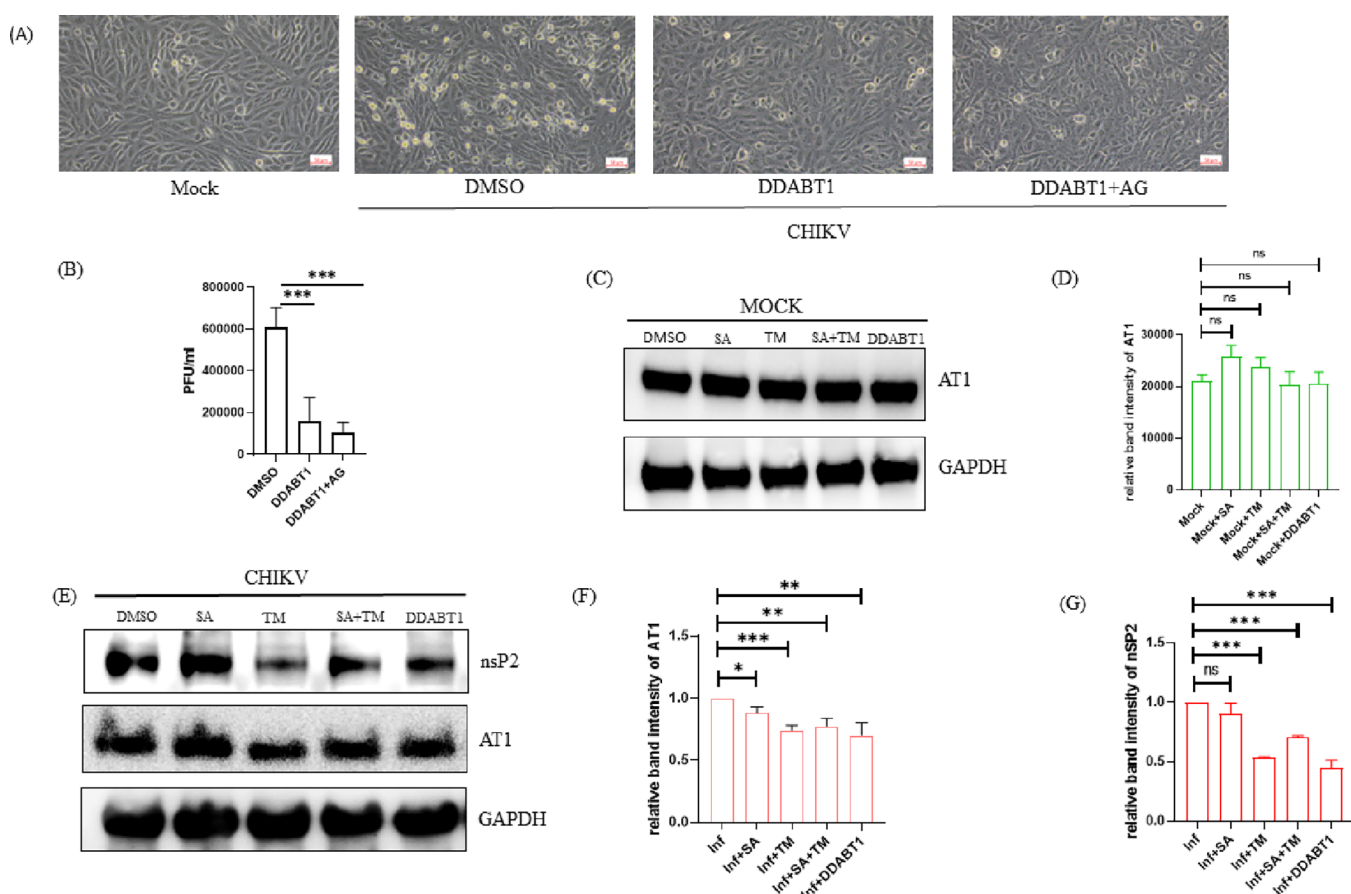
Figure 4. DDABT1 retains the ability of TM to inhibit AT1. Vero cells were infected with the CHIKV-PS strain of CHIKV (MOI 0.1) and then treated with DDABT1 (100 μM) along with AG (20 μM) after 90 min of infection. (A) Morphological changes in cells induced during infection at 18 hpi as observed under microscope at 10× magnification. (B) The bar graph shows the viral titer in PFU/ml. (C) Vero cells were treated with 50 μM doses of the compounds [SA/TM/SA+TM/DDABT1]. Cells were harvested at 18 hpi and Western blot was performed using AT1-specific mAb and GAPDH was taken as the loading control. (D) Bar graph showing the relative intensity of AT1 in different conditions of treatment. (E) Vero cells were infected with CHIKV-PS (MOI 0.1) for 90 min. The cells were then washed thrice with 1× PBS and 50 μM doses of the compounds [SA/TM/TM+SA/DDABT1] were added separately to the samples. Cells were harvested at 18 hpi, and Western blots were performed using AT1, nsP2 specific mAb, and GAPDH was taken as the loading control (F, G). Bar graph showing the relative intensity of AT1 and nsP2 in different conditions of infection and treatment. The statistical analysis of the experimental data was presented as mean ± SD of three independent experiments. *, $P \leq 0.05$; **, $P \leq 0.01$; ***, $P \leq 0.001$; and ****, $P \leq 0.0001$ were considered statistically significant.

The effect against chronic inflammation or arthritis was studied in the CFA-induced arthritis model in rats following established protocols.[26] Briefly, animals were grouped ($n = 6$) and pretreated with standard and test compounds as described earlier. Intraplantar injection of CFA (0.1 mL) in the left hind paw of the animals was used to induce arthritis. A vernier caliper (Mitutoyo, Japan) was used to measure the paw diameters at day 0 before CFA injections and thereafter on the 7th, 14th, 21st, and 28th days. The animals were treated with diclofenac, SA, SA+TM, and DDABT1 once daily during the observation periods. Blood samples (about 3 mL) were obtained by cardiac puncture on the 29th day and mixed with 3.8% sodium citrate solution in the proportion of four parts of blood to one part of the citrate solution. The erythrocyte sedimentation rate (ESR) was measured by Westergren's method,[27] whereas serum Rheumatoid Factor (RF) estimation was carried out by the turbidimetry method.[28] The arthritic limbs of the animals were maintained in 10% formalin for radiographic analysis.

2.13. Statistical Analysis. The data were presented as mean ± SD of three independent experiments and analyzed using the One-way ANOVA in the GraphPad Prism 5.0

software. The Bonferroni test was used for multiple comparisons. The P value of ≤ 0.05 was considered statistically significant.

3. RESULTS

3.1. Synthesis of DDABT1. The carboxylic acid group of SA was protected by benzylation before further reaction (I, Figure S1). Subsequently, the benzyl salicylate was esterified with TM (II, Figure S1). Finally, the benzyl group was removed by hydrogenolysis to yield DDABT1 (III, Figure S1). This was purified by column chromatography (*n*-hexane: ethyl acetate, 4:6 v/v) and recrystallized from ethanol. The purity was assessed by the HPLC method (retention time of 2.942 min with methanol as the mobile phase and 0.5 mL/min flow rate), (Figure S2a). The purity was calculated as a ratio of the area of the chromatogram to that of the total area and was found to be 96.5%. Based on the physicochemical properties (FTIR and NMR data), the structure of DDABT1 was proposed (III, Figure S1). The mass spectra showed the M-1 peak (Figure S2b) at 633.5 m/z, in confirmation of the proposed structure.

3.2. DDABT1 Inhibits CHIKV Infection More Efficiently than TM. The concentration of DDABT1 at which 50% of Vero cells were viable (CC_{50}) was found to be greater than 700 μM (Figure 1A). Since >95% of cells were viable at 100 μM concentration, DDABT1 was used at $\leq$100 μM in further experiments. Vero cells infected with CHIKV at MOI 0.1 were treated with the nontoxic concentrations of test compounds/drugs (50 μM of TM/SA/(TM+SA)/DDABT1) to assess the anti-CHIKV efficacy of DDABT1. The cells were observed for CHIKV-induced CPE under a bright field microscope, and supernatants were harvested at 18 hpi. It was observed that the reduction in CPE was more in the case of DDABT1 in comparison to either TM or its combination with SA (Figure 1B). The plaque assay revealed that the reduction in CHIKV progeny by DDABT1 (69%) was significantly higher than TM (43%), SA (7%), and their combinations (56%) (Figure 1C). Further, to estimate the concentration of DDABT1 that kills 50% of the virus (IC_{50}), Vero cells were infected with CHIKV (0.1 and 0.01 MOI), and different concentrations of DDABT1 (10−100 μM) were added to the cells postinfection. The IC_{50} of DDABT1 was found to be 21.07 and 14.59 μM for 0.1 and 0.01 MOI, respectively (Figure 1D). Hence, the result indicates that DDABT1 inhibits CHIKV infection more efficiently than TM.[16]

3.3. Post-Treatment of DDABT1 Reduces CHIKV Infection Significantly. CHIKV particles were incubated with DDABT1 for 30 min before infection to understand its potential to bind to the virus particle to prevent their entry into the host cells. The Vero cells were infected either with CHIKV or CHIKV incubated with DDABT1 (100 μM) for 90 min. Then, the cells were washed twice with 1× PBS before the addition of complete media. The cells and supernatants were harvested at 18 hpi. The plaque assay performed with the supernatant revealed no significant difference in viral titers between CHIKV and DDABT1 treated infected samples as shown in Figure 2A,C. This is also evident from the CPE results, as treatment before infection shows a CPE that is comparable to that of infection control (Figure 2B). Thus, the results indicate that DDABT1 does not inhibit CHIKV attachment and entry to the host cells. Treatment of DDABT1 during infection also failed to reduce CPE (Figure 2B) and viral titer (Figure 2D). However, postinfection treatment showed a significant reduction in CPE (Figure 2B) as well as in viral titer (75%) (Figure 2E). Further, the reduction in the viral proteins (Figure 2F−H) also confirmed the observation that post-treatment of DDABT1 can reduce CHIKV infection significantly.

3.4. Inhibition in CHIKV Progeny Release Even After the Addition of DDABT1 at 12 hpi. To find out the possible mechanism of action of DDABT1 on CHIKV replication, a time of addition experiment was performed. The Vero cells were infected with CHIKV-PS with MOI 0.1 and 100 μM of DDABT1 was added at 0, 2, 4, 6, 8, 10, and 12 hpi. The plaque assay showed >95% inhibition up to 4 hpi (Figure 3A). About 58% of the infectious virus particle release was abrogated, even after the addition of the drug at 12hpi. This indicates that DDABT1 predominantly inhibits the early stages of CHIKV infection; however, the late stages are also regulated significantly. Further, there was a significant reduction in CHIKV RNA (Figure 3B,C), and the viral proteins were remarkably decreased (Figure 3D−F). The data was further supported by an immunofluorescence assay where the number of E2-positive cells was reduced significantly

(Figure 3G,H). Thus, the result indicates that DDABT1 inhibits CHIKV RNA and protein levels significantly during infection *in vitro* in postcondition.

3.5. DDABT1 Retains the Ability of TM to Inhibit AT1. To understand whether DDABT1 retains the ability of TM to reduce AT1, Vero cells were infected with CHIKV-PS (MOI 0.1) and treated with DDABT1 (100 μM) along with AG (20 μM)). AG is known to augment AT1 expression and CHIKV infection that is antagonized by TM.[9] Like TM, DDABT1 reduced AG-mediated augmented CHIKV infection (Figure 4A,B) and AT1 expression (Figure 4C). Further, it also reduced the level of CHIKV nsP2 (Figure 4C). These results suggest that DDABT1 has the ability to inhibit CHIKV infection like TM by modulating the AT1.

3.6. DDABT1 Does Not Have Acute Oral Toxicity. An acute oral toxicity study revealed that there was no mortality up to a dose of 2000 mg/kg (Table S1). So, 5000 mg/kg was considered as LD_{50} (dose at which 50% of subject death occurs) according to the OECD-423 guideline. This revealed the safety level of the DDABT1. Thus, less than 1/100th LD_{50} (50 mg or 0.07 mmol/kg) was considered suitable for *in vivo* studies.

3.7. DDABT1 Shows Anti-Inflammatory Effects in Rats. The ability of test compounds to reduce edema/paw volume was expressed as a percentage of that of the control group. At the tested dose level (0.0194 mmol/kg), DDABT1 showed an 87.59% reduction in 4 h. This was higher than the inflammation inhibition shown by diclofenac (74.3%), SA (54.92%), or a combination of SA and TM (65.58%) (Figure 5A). This suggests that DDABT1 is capable of reducing acute inflammation in rats significantly. Further, DDABT1 showed 62.86 and 68.24% reduction in the weights of exudates and granuloma respectively in subacute inflammation studies (Figure 5B). This was comparable to that of diclofenac and significantly higher ($P < 0.01$) than that of a combination of TM and SA. In the CFA-induced arthritis model, diclofenac and DDABT1 showed 79.9 and 87.14% reduction, respectively, in paw edema on day 28. This was significantly ($p < 0.01$) higher than that of combinations of SA and TM (Figure 5C). In addition, treatment with DDABT1 showed the lowest levels of ESR (4.86 mm/h) and RF (10.83 IU/mL) (Figure 5D,E). The radiographic images of the affected limbs are shown in Figure 5F. The normal control (untreated) group of animals showed the absence of soft tissue swelling and narrowing of joint spaces. In CFA-induced arthritic rat, soft tissue swellings along with narrowing of the joint spaces were observed, which suggest bone destruction in arthritic conditions. The diclofenac-treated groups prevented this. Both the SA and TM-treated groups showed swelling of soft tissue and narrowing of the joint spaces. Whereas, treatment with their combination lowered this. DDABT1 minimized soft tissue swelling and joint space narrowing in rats. Taken together, these findings reveal that DDABT1 is effective against chronic inflammation/arthritis as compared to SA, TM, or their combination.

4. DISCUSSION

The DDABT1 was developed as an ester conjugate of TM and SA. The carboxylic acid group of SA was protected by benzylation (I, Figure S1) to avoid competition from the esterification of SA. The benzyl salicylate was further esterified to TM (II, Figure S1) by little modification of standard procedures.[15] In the final step, the protecting group (benzyl
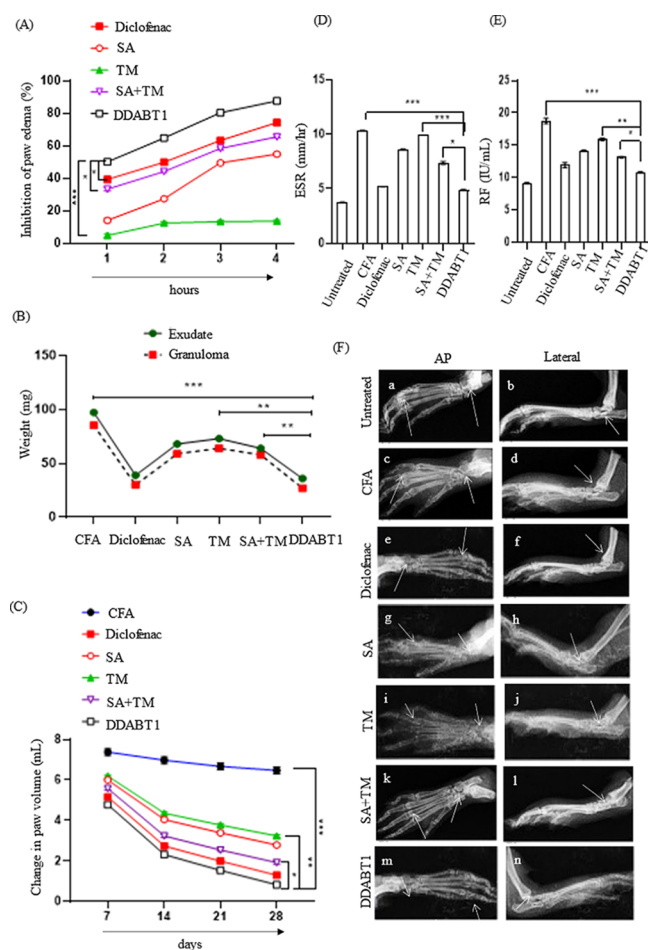
Figure 5. DDABT1 reduces adjuvant-induced arthritis and inflammation in rats. (A) Line diagram representing the acute anti-inflammatory effect. The data in the Y-axis represent the percentage of inhibition in paw edema induced by carrageenan injection in rat paws (an increase in paw edema of the control group is considered as 100%). (B) Line diagram depicting the subacute anti-inflammatory effect. Data in the Y-axis represent the weight of exudate in a cotton-pellet implanted model in rats. (C) The line diagram represents the effect against chronic inflammation. Data in the Y-axis represent the change in paw volume of rats compared to control following induction of arthritis and treatment. (D, E) The bar diagram shows levels of ESR and RF in animals following chronic inflammation (on the 29th day of induction of inflammation by CFA injection). (F) Radiographic images of hind limbs of rats to assess soft tissue swelling and bony destruction. The statistical analysis of the experimental data was presented as mean ± SD of six independent experiments. *, $P \leq 0.05$; **, $P \leq 0.01$; ***, $P \leq 0.001$; and ****, $P \leq 0.0001$ were considered statistically significant

alcohol) was removed by reduction to yield the DDABT1 (III, Figure S1). The purity of the compound was assessed to be 96.5% (Figure S2) and the proposed structure was supported by the physicochemical and spectral data.

The CC_{50} was found to be more than 700 μM and IC_{50} was 21.07 μM at 0.1 MOI. At this MOI TM is reported with an IC_{50} of 40.85.[10] Thus, conjugation to SA seems to have increased the potency against CHIKV. Moreover, the selectivity index of DDABT1 was found to be >33. In agreement with earlier reports, TM treatment reduced the viral titer.[9,10] The approved derivative of SA (acetyl salicylic) has been reported with antiviral effects against RNA viruses like human rhinovirus.[29] However, treatment with SA failed to

affect the viral titer of CHIKV. While its addition to TM made no significant difference in the viral titer, its conjugation to TM (DDABT1) enhanced the anti-CHIKV properties (Figure 1B). This encouraged further investigations.

As evident from the viral titer in CHIKV-infected and CHIKV + DDABT1 infected cells (Figure 2), it does not affect the CHIKV attachment to the host cells. Unlike TM[9], its treatment before infection failed to reduce CHIKV titer, whereas it was more effective in postinfection treatment. Accordingly, in postinfection stages, it decreased the RNA (nsP2 & E1) and protein expressions (nsP2 and E2) significantly (Figure 3). Recent studies have demonstrated that TM can bind to CHIKV-nsP2 and abrogate viral infection *in vitro*.[9,10] While the reduction in RNA level (nsP2) was comparable to that of TM, the reduction in the nsP2 protein level was relatively less. Nevertheless, a 70% reduction in the nsP2 level was observed by DDABT1. This can be attributed to the structural features of TM in DDABT1 (Table S2C). The time of addition experiment showed a significant reduction (approximately 95%) in viral titer following treatment with DDABT1 in the early stages (up to 4 hpi) of postentry infection. Compared to this, TM has been reported to be relatively more effective in the late stages (6−12 hpi) of infection (Table S2B). The variations in efficacy and stages of interference compared to TM may be due to any alteration in modes of action for DDABT1. Nonetheless, DDABT1 works in a similar way to TM by inhibiting AT1. However, this alone may not explain the mechanism of action of DDABT1, and further studies are necessary to validate this.

CHIKV-induced arthritis mimics the arthritis of the joints with a common pattern of inflammation[30] and drugs like diclofenac are used to manage these symptoms.[31] Thus, the results of a common model of inflammation and arthritis can be used to suggest the potential to manage CHIKV-induced arthritis. With this consideration, the anti-inflammatory effect of DDABT1 was evaluated in established animal models. The diclofenac, TM, and SA were used in human equivalent doses. Since DDABT1 is a conjugate of TM and SA, it was used at TM equivalent dose (0.0194 mmol/kg or 12 mg/kg) which is less than 1/100th of the LD_{50} dose (50 mg/kg). An increase in paw volume by carrageenan-induced paw edema in rats is a standard model of acute inflammation.[32] As is evident from the percentage reduction in paw edema (Figure 5A), DDABT1 showed a higher capacity to reduce acute inflammation. The cotton induced pellet-induced granuloma model in rats is used to measure subacute inflammation.[33] It represents the proliferative phase of the inflammation characterized by exudate production and formation of granulation tissue.[34] A 60% reduction in exudates and granulomatous tissue correlates well with the ability of DDABT1 to reduce inflammation. Further, it showed higher efficacy to reduce chronic inflammation compared to the diclofenac, SA, and TM as well as the combination of SA and TM (Figure 5D) in the CFA-induced arthritis model.[35] In support of these findings, DDABT1 was found to significantly reduce arthritis parameters including ESR and RF (Figure 5E). Compared to the combination of SA and TM, it was remarkably ($p < 0.05$) more effective. The higher efficacy of DDABT1 was also supported by the radiographic images (Figure 5F) that showed a reduction in soft tissue swelling and joint space narrowing. Thus, the ability to manage acute, subacute, and chronic inflammation suggests its potential to manage inflammation and arthritis associated with CHIKV infection. Thus, the

enhanced efficacy of DDABT1 to reduce CHIKV infection and arthritis compared to TM and SA justifies the hybridization of these molecules

In conclusion, the ability to inhibit CHIKV *in vitro* and inflammation/arthritis *in vivo* suggests the potential of DDABT1 to manage both the cause and symptoms of CHIKV infection. The conjugation of SA to TM was found to increase the efficacy. The anti-CHIKV property can be partly attributed to the ability of DDABT1 to reduce AT1. However, considering the fact that it also has features of salicylates, DDABT1 may have other modes of action and need further investigation. Also, evaluation in a preclinical-infection model is desirable to establish the antiviral property. Nonetheless, DDABT1 offers the prospect of an antiviral that can manage both the CHIKV infection and its symptoms simultaneously.

ASSOCIATED CONTENT

Supporting Information

The Supporting Information is available free of charge at https://pubs.acs.org/doi/10.1021/acsomega.3c00763.

Determination of oral acute toxicity of DDABT1 (SM1) and anti-inflammatory properties of DDABT1 (SM2); synthesis of DDABT1 (Figures S1 and S2); and acute oral toxicity of DDABT1 (Table S1), comparison between Telmisartan and DDABT1 (Table S2), and details of primers used (Table S3) (PDF)

AUTHOR INFORMATION

Corresponding Authors

Bharat B Subudhi − *Drug Development and Analysis Lab, School of Pharmaceutical Sciences, Siksha O Anusandhan Deemed to be University, Bhubaneswar 751003 Odisha, India;* orcid.org/0000-0002-2411-7292; Phone: +91-9853945363; Email: bharatbhusans@gmail.com

Soma Chattopadhyay − *Infectious Disease Biology, Institute of Life Sciences, Bhubaneswar 751023 Odisha, India;* orcid.org/0000-0001-8378-1014; Phone: +91-674-2304235; Email: sochat.ils@gmail.com

Authors

Rudra Narayan Dash − *Drug Development and Analysis Lab, School of Pharmaceutical Sciences, Siksha O Anusandhan Deemed to be University, Bhubaneswar 751003 Odisha, India;* orcid.org/0000-0002-9760-0808

Amrita Ray − *Infectious Disease Biology, Institute of Life Sciences, Bhubaneswar 751023 Odisha, India; Regional Centre for Biotechnology, 121001 Faridabad, India;* orcid.org/0000-0001-5220-9402

Prabhudutta Mamidi − *Infectious Disease Biology, Institute of Life Sciences, Bhubaneswar 751023 Odisha, India; Department of Microbiology (VRDL), AIIMS, Bhubaneswar 751019 Odisha, India*

Saikat De − *Infectious Disease Biology, Institute of Life Sciences, Bhubaneswar 751023 Odisha, India; Regional Centre for Biotechnology, 121001 Faridabad, India;* orcid.org/0000-0003-2028-0428

Tapas K Mohapatra − *Drug Development and Analysis Lab, School of Pharmaceutical Sciences, Siksha O Anusandhan Deemed to be University, Bhubaneswar 751003 Odisha, India; Nityananda College of Pharmacy, Balasore, Odisha 756060, India;* orcid.org/0000-0003-4754-8973

Alok K Moharana − *Drug Development and Analysis Lab, School of Pharmaceutical Sciences, Siksha O Anusandhan Deemed to be University, Bhubaneswar 751003 Odisha, India; School of Pharmacy, Arka Jain University, Mohanpur, Jharkhand 832108, India;* orcid.org/0000-0002-6169-6000

Tathagata Mukherjee − *School of Biological Sciences, National Institute of Science Education and Research, HBNI, 752050 Bhubaneswar, India;* orcid.org/0000-0001-7504-5957

Soumyajit Ghosh − *Infectious Disease Biology, Institute of Life Sciences, Bhubaneswar 751023 Odisha, India; Regional Centre for Biotechnology, 121001 Faridabad, India;* orcid.org/0000-0003-3991-3010

Subhasis Chattopadhyay − *School of Biological Sciences, National Institute of Science Education and Research, HBNI, 752050 Bhubaneswar, India;* orcid.org/0000-0002-2596-8451

Complete contact information is available at:
https://pubs.acs.org/10.1021/acsomega.3c00763

Author Contributions

○R.N.D., A.R., and P.M. contributed equally to this work.

Author Contributions

S.C., B.B.S., R.N.D., A.R., P.M. conceived the idea, designed the experiments, and analyzed the results; S.C., B.B.S. contributed reagents; R.N.D., A.R., P.M., S.D., T.K.M., A.K.M., S.G., and T.M. carried out the experiments; S.D. carried out visualization of the data; and A.R., P.M., S.D., S.C., B.B.S., and S.C. wrote and edited the manuscript. S.C. and B.B.S. reviewed the manuscript. All the authors approved the final manuscript.

Notes

The authors declare no competing financial interest.

ACKNOWLEDGMENTS

■ DEDICATION

■ REFERENCES

(1) Weaver, S. C.; Lecuit, M. Chikungunya virus and the global spread of a mosquito-borne disease. *N Engl J. Med.* **2015**, *372* (13), 1231−1239. Simon, F.; Javelle, E.; Cabie, A.; Bouquillard, E.; Troisgros, O.; Gentile, G.; Leparc-Goffart, I.; Hoen, B.; Gandjbakhch, F.; Rene-Corail, P.; et al. French guidelines for the management of chikungunya (acute and persistent presentations). November 2014. *Med. Mal Infect* **2015**, *45* (7), 243−263.

(2) Cunha, R. V. D.; Trinta, K. S. Chikungunya virus: clinical aspects and treatment - A Review. *Mem Inst Oswaldo Cruz* **2017**, *112* (8), 523−531.

(3) Queyriaux, B.; Simon, F.; Grandadam, M.; Michel, R.; Tolou, H.; Boutin, J. P. Clinical burden of chikungunya virus infection. *Lancet Infect Dis* **2008**, *8* (1), 2−3.

(4) Morrison, T. E. Reemergence of chikungunya virus. *J. Virol* **2014**, *88* (20), 11644−11647.

(5) Kumar, A.; Mishra, P.; Chattopadhyay, S.; Subudhi, B. B. Current Strategies for Inhibition of Chikungunya Infection. *Viruses* **2018**, *10* (5), 235. Kovacikova, K.; van Hemert, M. J. Small-Molecule Inhibitors of Chikungunya Virus: Mechanisms of Action and Antiviral Drug Resistance. *Antimicrob. Agents Chemother.* **2020**, *64* (12), No. e01788-20.

(6) Blakely, P. K.; Huber, A. K.; Irani, D. N. Type-1 angiotensin receptor signaling in central nervous system myeloid cells is pathogenic during fatal alphavirus encephalitis in mice. *J. Neuroinflammation* **2016**, *13* (1), 196.

(7) Hernandez-Fonseca, J. P.; Duran, A.; Valero, N.; Mosquera, J. Losartan and enalapril decrease viral absorption and interleukin 1 beta production by macrophages in an experimental dengue virus infection. *Arch. Virol.* **2015**, *160* (11), 2861−2865.

(8) Huang, F.; Guo, J.; Zou, Z.; Liu, J.; Cao, B.; Zhang, S.; Li, H.; Wang, W.; Sheng, M.; Liu, S.; et al. Angiotensin II plasma levels are linked to disease severity and predict fatal outcomes in H7N9-infected patients. *Nat. Commun.* **2014**, *5*, 3595.

(9) De, S.; Mamidi, P.; Ghosh, S.; Keshry, S. S.; Mahish, C.; Pani, S. S.; Laha, E.; Ray, A.; Datey, A.; Chatterjee, S.; et al. Telmisartan Restricts Chikungunya Virus Infection In Vitro and In Vivo through the AT1/PPAR-gamma/MAPKs Pathways. *Antimicrob. Agents Chemother.* **2022**, *66* (1), No. e0148921.

(10) Tripathi, P. K.; Soni, A.; Singh Yadav, S. P.; Kumar, A.; Gaurav, N.; Raghavendhar, S.; Sharma, P.; Sunil, S.; Ashish; Jayaram, B.; et al. Evaluation of novobiocin and telmisartan for anti-CHIKV activity. *Virology* **2020**, *548*, 250−260.

(11) Singh, D. P.; Moore, C. A.; Gilliland, A.; Carr, J. P. Activation of multiple antiviral defence mechanisms by salicylic acid. *Mol. Plant Pathol* **2004**, *5* (1), 57−63.

(12) Steer, S. A.; Corbett, J. A. The role and regulation of COX-2 during viral infection. *Viral Immunol.* **2003**, *16* (4), 447−460.

(13) Chattopadhyay, S.; Kumar, A.; Mamidi, P.; Nayak, T. K.; Das, I.; Chhatai, J.; Basantray, I.; Bramha, U.; Maiti, P. K.; Singh, S.; et al. Development and characterization of monoclonal antibody against non-structural protein-2 of Chikungunya virus and its application. *J. Virol. Methods* **2014**, *199*, 86−94.

(14) Furniss, B. S.; Hannford, A. J.; Smith, P. W. G.; Tatchell, A. R. *Vogel's Textbook of Practical Organic Chemistry*; 1988.

(15) Subudhi, B. B.; Sahu, P. K.; Singh, V. K.; Prusty, S. Conjugation to Ascorbic Acid Enhances Brain Availability of Losartan Carboxylic Acid and Protects Against Parkinsonism in Rats. *AAPS J.* **2018**, *20* (6), 110. Neises, W. S. B. Simple Method for the Esterification of Carboxylic Acids. *Angew. Chem., Int. Ed.* **1978**, *17* (7), 522−524.

(16) De, S.; Ghosh, S.; Keshry, S. S.; Mahish, C.; Mohapatra, C.; Guru, A.; Mamidi, P.; Datey, A.; Pani, S. S.; Vasudevan, D.; et al.

MBZM-N-IBT, a Novel Small Molecule, Restricts Chikungunya Virus Infection by Targeting nsP2 Protease Activity In Vitro, In Vivo, and Ex Vivo. *Antimicrob. Agents Chemother.* **2022**, *66* (7), No. e0046322.

(17) Kumar, A.; Mamidi, P.; Das, I.; Nayak, T. K.; Kumar, S.; Chhatai, J.; Chattopadhyay, S.; Suryawanshi, A. R.; Chattopadhyay, S. A novel 2006 Indian outbreak strain of Chikungunya virus exhibits different pattern of infection as compared to prototype strain. *PLoS One* **2014**, *9* (1), No. e85714.

(18) Mishra, P.; Kumar, A.; Mamidi, P.; Kumar, S.; Basantray, I.; Saswat, T.; Das, I.; Nayak, T. K.; Chattopadhyay, S.; Subudhi, B. B.; et al. Inhibition of Chikungunya Virus Replication by 1-[(2-Methylbenzimidazol-1-yl) Methyl]-2-Oxo-Indolin-3-ylidene] Amino] Thiourea(MBZM-N-IBT). *Sci. Rep* **2016**, *6*, 20122.

(19) Nath, P.; Chauhan, N. R.; Jena, K. K.; Datey, A.; Kumar, N. D.; Mehto, S.; De, S.; Nayak, T. K.; Priyadarsini, S.; Rout, K.; et al. Inhibition of IRGM establishes a robust antiviral immune state to restrict pathogenic viruses. *EMBO Rep* **2021**, *22* (11), No. e52948.

(20) Das, I.; Basantray, I.; Mamidi, P.; Nayak, T. K.; B, M. P.; Chattopadhyay, S.; Chattopadhyay, S. Heat shock protein 90 positively regulates Chikungunya virus replication by stabilizing viral non-structural protein nsP2 during infection. *PLoS One* **2014**, *9* (6), No. e100531.

(21) Sanjai Kumar, P.; Nayak, T. K.; Mahish, C.; Sahoo, S. S.; Radhakrishnan, A.; De, S.; Datey, A.; Sahu, R. P.; Goswami, C.; Chattopadhyay, S.; et al. Inhibition of transient receptor potential vanilloid 1 (TRPV1) channel regulates chikungunya virus infection in macrophages. *Arch. Virol.* **2021**, *166* (1), 139−155.

(22) Mamidi, P.; Nayak, T. K.; Kumar, A.; Kumar, S.; Chatterjee, S.; De, S.; Datey, A.; Ghosh, S.; Keshry, S. S.; Singh, S.; et al. MK2a inhibitor CMPD1 abrogates chikungunya virus infection by modulating actin remodeling pathway. *PLoS Pathog* **2021**, *17* (11), No. e1009667.

(23) Kumar, A.; De, S.; Moharana, A. K.; Nayak, T. K.; Saswat, T.; Datey, A.; Mamidi, P.; Mishra, P.; Subudhi, B. B.; Chattopadhyay, S. Inhibition of herpes simplex virus-1 infection by MBZM-N-IBT: in silico and in vitro studies. *Virol J.* **2021**, *18* (1), 103.

(24) Phyllis, E.; Whiteley, S. A. D. Models of Inflammation: Carrageenan-Induced Paw Edema in the Rat. In *Current protocols in pharmacology*; 2001.

(25) D'Arcy, P. F.; Howard, E. M.; Muggleton, P. W.; Townsend, S. B. The anti-inflammatory action of griseofulvin in experimental animals. *J. Pharm. Pharmacol* **2011**, *12*, 659−665.

(26) Chillingworth, N. L.; Donaldson, L. F. Characterisation of a Freund's complete adjuvant-induced model of chronic arthritis in mice. *J. Neurosci Methods* **2003**, *128* (1−2), 45−52. Snekhalatha, U.; Anburajan, M.; Venkatraman, B.; Menaka, M. Evaluation of complete Freund's adjuvant-induced arthritis in a Wistar rat model. Comparison of thermography and histopathology. *Z. Rheumatol* **2013**, *72* (4), 375−382.

(27) Mehta, A.; Sethiya, N. K.; Mehta, C.; Shah, G. B. Anti-arthritis activity of roots of Hemidesmus indicus R.Br. (Anantmul) in rats. *Asian Pac. J. Trop Med.* **2012**, *5* (2), 130−135.

(28) Asquith, D. L.; Miller, A. M.; McInnes, I. B.; Liew, F. Y. Animal models of rheumatoid arthritis. *Eur. J. Immunol.* **2009**, *39* (8), 2040−2044.

(29) Glatthaar-Saalmuller, B.; Mair, K. H.; Saalmuller, A. Antiviral activity of aspirin against RNA viruses of the respiratory tract-an in vitro study. *Influenza Other Respir Viruses* **2017**, *11* (1), 85−92.

(30) Amdekar, S.; Parashar, D.; Alagarasu, K. Chikungunya Virus-Induced Arthritis: Role of Host and Viral Factors in the Pathogenesis. *Viral Immunol* **2017**, *30* (10), 691−702.

(31) Pathak, H.; Mohan, M. C.; Ravindran, V. Chikungunya arthritis. *Clin Med. (Lond)* **2019**, *19* (5), 381−385.

(32) Morris, C. J. Carrageenan-induced paw edema in the rat and mouse. *Methods Mol. Biol.* **2003**, *225*, 115−121.

(33) Kumar, R.; Gupta, Y. K.; Singh, S. Anti-inflammatory and anti-granuloma activity of Berberis aristata DC. in experimental models of inflammation. *Indian J. Pharmacol* **2016**, *48* (2), 155−161.

(34) Afsar, S.K.; Kumar, K. R.; Gopal, J. V.; Raveesha, P. Assessment of anti-inflammatory activity of Artemisia vulgaris leaves by cotton pellet granuloma method in Wistar albino rats. *J. Pharm. Res.* **2013**, 7 (6), 463−467.

(35) Li, Y.; Kakkar, R.; Wang, J. In vivo and in vitro Approach to Anti-arthritic and Anti-inflammatory Effect of Crocetin by Alteration of Nuclear Factor-E2-Related Factor 2/hem Oxygenase (HO)-1 and NF-kappaB Expression. *Front Pharmacol* **2018**, 9, 1341. Mahdi, H. J.; Khan, N. A. K.; Asmawi, M. Z. B.; Mahmud, R.; V, A. L. M. In vivo anti-arthritic and anti-nociceptive effects of ethanol extract of Moringa oleifera leaves on complete Freund's adjuvant (CFA)-induced arthritis in rats. *Integr. Med. Res.* **2018**, 7 (1), 85−94.